Advanced Production and Industrial Engineering
R.M. Singari and P.K. Kankar (Eds.)

doi:10.3233/ATDE220752

Numerical Modelling and Simulation of μ-EDM Process on Inconel 718 Using FEM Model

Souradeep DUTTA[a,1], Dr. Deba Kumar SARMA[a], Dr. Koushik DAS[a], Bhargab Madhab BARUA[a]
[a] *Department of Mechanical Engineering, National Institute of Technology Meghalaya, Shillong, 793003, India*

Abstract. Nickle based super alloy Inconel 718 is a difficult to cut material due to its large mechanical strength and high heat and corrosion resistance with good thermal stability. μ-EDM is a non-conventional micro-machining process that can produce complex micro features in Inconel 718. The material removal mechanism of μ-EDM is extremely intricate and dynamic in nature. This paper aims to develop a 2D axisymmetric heat transient model that can explain the material removal theory during the single spark μ-EDM process on Inconel 718. The solutions of the developed model have been obtained by finite element method (FEM) based software COMSOL Multiphysics 5.6. First, the model is validated with a literature model by incorporating the same machining condition. It has been accomplished that the present model's crater radius (r') and depth (h) values are in a close agreement with the literature model. The absolute percentage error for r' and h between the simulated results of the two models are found to be 1.37 and 4.45 correspondingly. Both the r' and h are increased with the enhancement of discharge energy (DE). The highest value of r' and h are found at 7.2 μJ DE followed by 6.05 μJ and 5 μJ DE. It has been established that the temperature has been drastically decreased along both the radius and depth direction after the single spark simulation process. The temperature gradient is found to be more along the radius direction than the depth direction.

Keywords. μ-EDM, simulation, crater radius, crater depth, discharge energy.

1. Introduction

Nickel based super alloy Inconel 718 is widely utilized in the aerospace industry for its high mechanical strength, high corrosion and heat resistance and improved thermal stability [1]. Conventional machining is quite difficult to process Inconel 718 because of that non-convention machining such as μ-EDM has been considered in this study [2]. A numerical model was constructed for modelling of single-discharge μ-EDM on titanium alloy. FEM analysis revealed the crater's diameter-to-depth ratios to be 3.45 and 3.99, for titanium alloy correspondingly [3]. A 3D FVM method is provided as another addition to the modelling and simulation of the sophisticated μ-EDM operation. The

[1]Corresponding author, Souradeep Dutta, Department of Mechanical Engineering, National Institute of Technology, Meghalaya, Email: Souradeepdutta.73@gmail.com

results of the generated model were found to be quite close to the experimental results for crater size and temperature distribution [4]. A new meshless method named Meshless Local Petro-Galerkin (MLPG) and Element Free Galerkin Method (EFGM) is applied for solving for solving electrostatic problems. These two methods give faster and accurate results and able to replace FEM [5]. A brief review was carried out for various meshless methods used for different structural problems. It was found that MLPG and EFGM can be applied to solve complex problems and overcome the limitations of FEM [6]. Based on the literature available, it is noticed that very less studies are told about the single discharge modelling of μ-EDM operation on Inconel 718. The present study deals with the single spark numerical simulation of μ-EDM process by taking Gaussian heat flux distribution in a 2D axisymmetric heat transient model on Inconel 718 super alloy. At first, the developed model is validated with the previous literature model. Then the crater dimensions are measured by linier interpolation method after the simulation in COMSOL Multiphysics FEM software. The variation of r' and h with the DE is accomplished in the present study. The temperature profile along the radius and depth are also discussed in the present research.

2. Illustration of the μ-EDM model

In EDM a high potential difference is given between the cathode (tool) and anode (workpiece) immersed in dielectric media. The electrons are ejected at a high rate towards the anode, while the ions are ejected towards the cathode. The dielectric molecules are ionized as a result of this movement, and a plasma channel is formed. Due to the breakdown of the dielectric fluid the temperature around the plasma channel becomes very high (more than 10000ºC) which melts and vaporizes the workpiece material. The thermal erosion process in EDM removes the material. The principle is same in μ-EDM only at a very small gap size and small discharge duration with a higher energy density. Some assumptions are listed below to simplify the thermal model of μ-EDM.

2.1 Assumptions

The material is considered to be isotropic and homogeneous with faces except the top face remains insulated. Heat transfer occurs by conduction mode up to the spark radius and after that convection heat transfer takes place. Single pulse single spark with 100% flushing efficiency is considered. Specific heat capacity, density and thermal conductivity of the material remained constant.

2.2 Physical description and boundary condition

A 2D axisymmetric domain is considered for single discharge modelling of μ-EDM operation which is elaborated in Figure 1. The Fourier heat conduction equation is considered as the governing equation in cylindrical coordinate system. The governing equation applied for the single-discharge numerical analysis in μ-EDM is given as-

$$\frac{1}{r}\frac{\partial}{\partial r}\left(r\frac{\partial T}{\partial r}\right)+\frac{\partial^2 T}{\partial z^2}=\frac{1}{\alpha}\frac{\partial T}{\partial t} \tag{1}$$

where r and z are the directions in both axis, T is the temperature, and α is the thermal diffusivity of the workpiece material. The analytical solution of equation (1) gives the temperature variation along the radial and depth on the surface of the workpiece.
The heat transfer boundary condition (boundary 1) is described as $-k\frac{\partial T}{\partial y}=q_x,(\text{for } r \le R)$ and $-k\frac{\partial T}{\partial y}=\hbar(T-T_\infty)(\text{for } r>R)$. Here, R is the spark radius. $\hbar$ is the convection heat transfer coefficient of the dielectric fluid. T_∞ of 298 K is taken as the dielectric fluid temperature. As there is no heat loss in boundary 3 and 4, they remain insulated $(-k\nabla T=0)$ for the analysis.

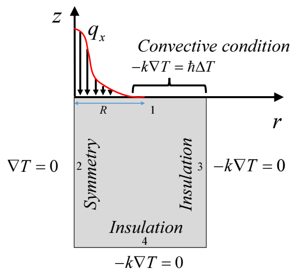

Figure 1. Schematic diagram of the 2D axisymmetric thermal model with boundary condition

Based on the study of the previous researchers Gaussian heat distribution is taken into consideration [7]. According to [7] the heat flux density rate was given by $q_x=q_0\exp\left[-4.5\left(\frac{r}{R}\right)^2\right]$. Here, q_x is the heat flux density rate in W/m^2, q_0 is the maximum amount of heat generated in the workpiece. The maximum amount of heat generated is given by $q_0=4.57\frac{\eta E}{t_{on}\pi R^2}$ [8]. The $E\left(=\frac{1}{2}CV^2\right)$ is the DE and t_{on} is the pulse on time. The η (= 0.39) is defined as the fraction of DE per pulse, which is assigned to the workpiece. The C and the V represents the capacitance and voltage. As spark radius is not constant, so it varies with time according to $R=0.0284(t_{on})^{0.9115}$ [9]. Here t_{on} is in nanoseconds and R is in μm.

3. Results and discussions

The detailed results and discussion section comprise of following subsections which is given below –

3.1 Model Validation

At first, the present model is validated with the simulated and experimental results of Dilip et al., 2020 [10] termed as literature model in order to assess its accuracy. The simulation is carried out with the same machining condition of [10] during single spark μ-EDM process. The machining variables used for the validation and as well as simulation is depicted in Table 1. Finite volume method (FVM) has been applied to determine the r' and h in the study of [10] which is carried out MATLAB software. The present model determines the r' and h value by FEM which is carried out in COMSOL Multiphysics 5.6 software. 1st order free triangular elements are used in the present study. The no of elements is more in the region of heat flux radius and it decreases gradually towards the rest of the region. The minimum and maximum element size has been taken as 0.0375 μm and 10 μm accordingly. The obtained values of r' and h are compared with the simulated and experimental values of [10] given in Table 2. The absolute percentage error of r' and h between the two simulated results have been found to be 1.37 and 4.45. It is noticed that both the percentage errors are ascertain to be less than 5%. It shows that the prediction capability of the developed present model is quite high. It is also noticed that both the r' and h values obtained by the present model is comparatively closer to the experimental values of the literature model [10]. The absolute percentage error of r' and h between the experimental results of [10] and the simulated results of the present model have been found to be 5.40 and 17.70 correspondingly.

Table 1. Machining variables

Pulse on time (t_{on})	: 3 μs	Thermal conductivity (k)	: 11.4 W/m K
Pulse off time (t_{off})	: 10 μs	Specific heat (C_p)	: 435 J/kg K
Gap Voltage	: 100 V (for validation), 110, 120 V	Melting temperature	: 1609 K
Capacitance	: 0.4 μF (for validation), 0.001 μF	Discharge energy (DE)	: 5,6.05 and 7.2 μJ
Film coefficient ($\hbar$)	: 1000 W/m^2 K	Density (ρ)	: 8190 kg/m^3

The simulated r' and h values have been established to be less when compared with the experimental values of [10]. This is due to the assumption of 100% flushing efficiency. All the molten alloys are not evaporated during the actual μ-EDM operation and there is a recast layer formed after the single spark μ-EDM process. It reduces the crater's actual size in comparison to the simulated size.

Table 2. Comparison of crater radius and depth between the literature model and present model at a capacitance of 0.4 μF and gap voltage of 100 V

Parameter	Results from Literature [10]		Present numerical result	% Error between of the present result with [10] data obtained	
	Numerical	Experimental		Numerically	Experimentally
r' (μm)	29.85	27.93	29.44	1.37	5.40
h (μm)	11.9	9.66	11.37	4.45	17.70

3.2 *Parametric study of crater radius and depth with DE*

The numerical modelling of the single discharge μ-EDM model is carried out on COMSOL Multiphysics 5.6 software. Less than 10% of the domain size is considered the spark or heat flux radius where the conduction mode of heat transfer occurred. Free triangular mesh (minimum mesh size 0.15 μm) is considered for the present study. The gap voltages are selected based on the literature survey and expert opinion. The mesh size is gradually increased from the spark radius section where the crater formed to the remaining section of the domain. After incorporating all the boundary conditions and applying the Gaussian distribution of heat flux, the craters are generated at 5 μJ, 6.05μJ and 7.2μJ DE as shown in Figure 2(a-c). An assumption is made that all the portion of Inconel 718 is removed when the temperature exceeds the melting point (1609 K) (100% flushing efficiency). It has been noticed that hemispherical shaped craters are generated for each DE after the simulation process. The r' and h values are measured in the direction of r and z axis upto the melting point zone by linier interpolation.

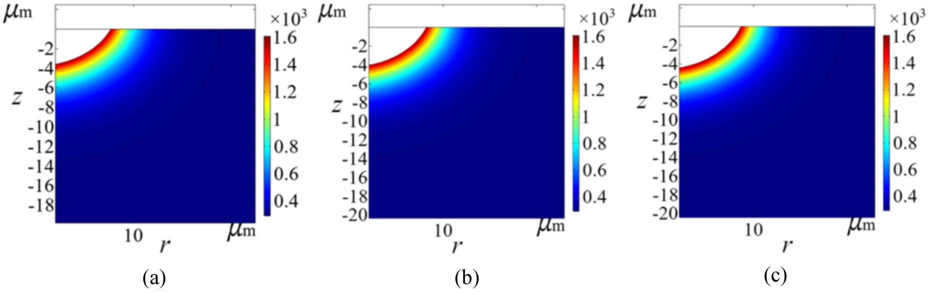

Figure 2. Crater radius and depth simulated at (a) 5 μJ DE (b) 6.05 μJ DE and (c) 7.2 μJ DE

The r' and h against each DE is given in Table 3. The crater dimensions are directly depending upon the DE per pulse. The r' and h are enhanced with the increase of DE in a very sharp manner. The enhancement of DE increases the heat flux density rate, generating higher temperature in the workpiece. The higher the temperature, the more material is removed per pulse, resulting in a larger value of r' and h. Due to that reason, the r' and h are much higher in 7.2 μJ DE than the 5 μJ DE.

Table 3. Crater dimensions obtained from single spark simulation for different machining condition

Sl. no	V(Volt)	C (pF)	DE (μJ)	r' (μm)	h (μm)
1	100		5	7.59	3.74
2	110	1000	6.05	8.12	4.19
3	120		7.2	8.57	4.57

3.3 Temperature distribution along the r and z direction

The temperature variation with different discharge energies (5μJ, 6.05μJ and 7.2 μJ) along the r and z of the job is shown in Figure 3 and 4. It is noticed that the temperature drastically decreases along both the r and z. The maximum temperature is found in the origin of the job. Gaussian distribution of heat flux is responsible for this kind of temperature profile. As the heat transfer is carried out by conduction mode until plasma radius, the temperature decreases rapidly from the top edge to the spark radius and further it remains constant due to convective heat transfer with the ambient. The temperature generated after each spark is truly relies upon the given DE. Due to that, the highest temperature 8200 K is generated at 7.2 μJ DE followed by 6900 K at 6.05 μJ DE and 5700 K at 7.2 μJ DE. It is also noticed that the temperature gradient is more along the r direction than the workpiece's z direction. It occurs because to a lack of direct heat flow in the workpiece's z direction.

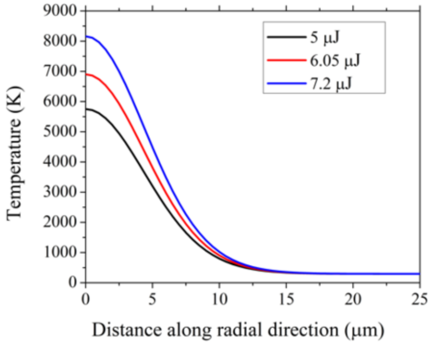

Figure 3. Temperature distribution at various DE along the radial direction

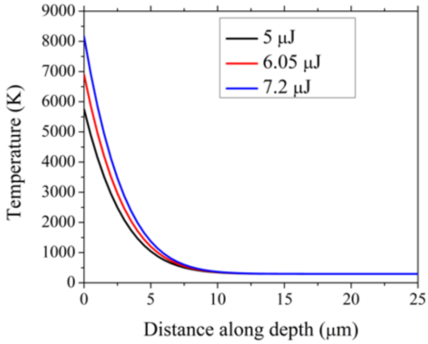

Figure 4. Temperature distribution at various DE along the depth

4. Conclusions

The detected crater radius and depth values are found to be quite close to the literature model with absolute percentage error of 1.37 and 4.45 respectively during single spark simulation of μ-EDM process on Inconel 718. The highest temperature has been developed during 7.2 μJ DE followed by 6.05 μJ and 5 μJ along both the radius and depth direction during single spark simulation of μ-EDM process. Larger crater radius and depth values are found at 7.2 μJ DE followed by 6.05 μJ and 5 μJ DE. The present model can be converted to more realistic model by considering variable flushing efficiency and recast layer formation along with μ-EDM experimentation.

References

[1] Dudzinski D, Devillez A, Moufki A, Larrouquere D, Zerrouki V, Vigneau J. A review of developments towards dry and high speed machining of Inconel 718 alloy. Int J Mach Tools Manuf. 2004 March;45(4):1353-67.

[2] Ho KH, Newman ST. State of the art in electrical discharge machining (EDM). Int J Mach Tools Manuf. 2003 Oct;43(13):1287-1300.

[3] Murali MS, Yeo SH. Process simulation and residual stress estimation of micro electric discharge machining using finite element method. J Appl Phys. 2005 Jul;44(7A):5254–63.

[4] Kuriachen B, Varghese A, Somashekhar KP. Panda S. Mathew J. Three-dimensional numerical simulation of microelectric discharge machining of Ti-6Al-4V. Int J Adv Manuf Technol. 2015 Jan;79: 147–160.

[5] Kumar M, Rajiyan J, Gupta P. A computational approach for solving elasto-statics problems. Mater Today: Proc. 2021 May;46:6876-79.

[6] Kumar M, Jha AK, Bhagoria Y, Gupta P. A review to explore different meshless methods in various Structural problems. IOP Conf. Ser.: Mater. Sci. Eng. 2021; 1116:012119.

[7] Joshi SN, Pande SS. Thermo-physical modeling of diesinking EDM process. J Manuf Process. 2010 Jan;12(1):45–56.

[8] Singh M, Saxena P, Ramkumar J, Rao RV. Multi-spark numerical simulation of the micro-EDM process: an extension of a single-spark numerical study. Int J Adv Manuf Technol. 2020 June;108:2701–15.

[9] Yeo SH, Kurnia W, Tan PC. Electro thermal modeling of anode and cathode in micro EDM. J Phys D. 2007 Apr;40(8):2513.

[10] Dilip DG, John G, Panda S. Mathew J. Finite-volume-based conservative numerical scheme in cylindrical coordinate system to predict material removal during micro-EDM on Inconel 718. J Braz Soc Mech Sci Eng. 2020 Jan;42:90.